Earth Planets Space, **61**, 119–124, 2009

Grain size dependence of low-temperature remanent magnetization in natural and synthetic magnetite: Experimental study

Aleksey V. Smirnov

Department of Geological and Mining Engineering and Sciences, Michigan Technological University, Houghton, MI 49931, USA

(Received December 28, 2007; Revised February 29, 2008; Accepted March 11, 2008; Online published January 23, 2009)

Magnetic measurements at cryogenic temperatures (<300 K) proved to be useful in paleomagnetic and rock magnetic research, stimulating continuous interest to low-temperature properties of magnetite and other magnetic minerals. Here I report new experimental results on a grain size dependence of the ratio (R_{LT}) between a low-temperature (20 K) saturation isothermal remanent magnetization (SIRM) imparted in magnetite after cooling in a 2.5 T field (field cooling, FC) and in a zero field environment (zero field cooling, ZFC). Synthetic magnetite samples ranged in mean grain size from 0.15 to 100 μm, representing nearly single-domain (SD), pseudosingle-domain (PSD), and multidomain (MD) magnetic states. The R_{LT} ratio monotonically increases from 0.58 to 1.12 with the decreasing mean grain size, being close to unity for PSD grains (0.15–5 μm) and smaller than unity for MD magnetite (12–100 μm). The R_{LT} ratio of 1.27 is observed for acicular magnetite characterized by nearly SD behavior. These observations indicate that within the range of ~0.15 to ~5 μm, the low-temperature SIRM may be higher than that expected from "normal" magnetic domain wall displacement. Such a behavior can be caused by the presence of a SD-like component in the magnetization of these grains, which origin, however, is uncertain. The natural rocks containing nearly stoichiometric magnetite manifest a dependence of the R_{LT} ratio on magnetic domain state identical to that observed from synthetic magnetites. Therefore, the comparison of FC SIRM and ZFC SIRM at very low temperatures may allow a crude estimate of magnetic domain state in some magnetite-bearing rocks, such as shallow mafic intrusions or some marine sediments.

Key words: Magnetite, Verwey transition, twinning, remanent magnetization, zero field cooling.

1. Introduction

Magnetite (Fe_3O_4) occurs in a great variety of igneous, sedimentary, and metamorphic rocks, and is one of the principal recorders of paleomagnetic and paleointensity information on the Earth (e.g., Dunlop and Özdemir, 1997) and, potentially, other planets (e.g., Arkani-Hamed, 2005). The grain size distribution, oxidation state, and morphology of natural magnetite have been utilized as proxies of climatic, environmental, and biogeochemical processes (e.g., Kirschvink and Lowenstam, 1979; Geiss *et al.*, 2004; Kopp *et al.*, 2007).

Magnetite is easily distinguishable by its peculiar physical properties at cryogenic temperatures (<300 K) characterized by two low-temperature transitions. The first transition (the isotropic point, T_i) occurs at ~130 K, when the first magnetocrystalline constant passes through zero and changes sign (e.g., Syono, 1965) and the easy magnetization axes change their orientation from [111] above T_i to [100] below T_i (e.g., Stacey and Banerjee, 1974). On further cooling, at ~120 K, magnetite undergoes a phase transition from cubic to lower (probably monoclinic (Zuo *et al.*, 1990)) crystalline symmetry at ~120 K (T_V, the Verwey transition) (Verwey, 1939). The Verwey transition is accompanied by a change in magnetocrystalline anisotropy from cubic to uniaxial, when one of the cubic [100] directions becomes the monoclinic c-axis (e.g., Kakol, 1990), which is a new easy magnetization axis. As a result of this change, a reorganization of the domain structure is expected upon passing through the transition (e.g., Halgedahl and Jarrard, 1995). Lowering of crystal symmetry below T_V results in the appearance of ferroelastic domains, or twins, to reduce spontaneous strain (e.g., Chikazumi *et al.*, 1971; Medrano *et al.*, 1999). Within a ferroelastic domain, the direction of c-axis is constant. Twinning appears to play an important role in determining magnetic properties of magnetite below T_V (e.g., Özdemir and Dunlop, 1999; Kosterov, 2001; Smirnov and Tarduno, 2002).

The Verwey transition is accompanied by abrupt changes of magnetic properties depending on magnetocrystalline anisotropy, such as remanent magnetization (e.g., Özdemir *et al.*, 1993, 2002). In particular, a saturation isothermal remanent magnetization (SIRM) imparted in magnetite at room temperature or at a very low temperature sharply decreases upon cooling or warming through T_V, respectively. The characteristic SIRM decrease has been commonly used for magnetite identification in synthetic and natural samples (e.g., Dunlop and Özdemir, 1997).

It has been long known that magnetic properties of magnetite below T_V are controlled by the strength of a magnetic field applied during cooling through the transition (e.g., Li, 1932; Bickford, 1950; Williams *et al.*, 1953; Schmidbauer and Keller, 1996; Kosterov, 2001; Smirnov, 2006).

Table 1. Grain-size distribution and room-temperature magnetic hysteresis characteristics of the samples studied. Parameters d_{mode}, d_{lower}, and d_{upper} characterize the observed distributions. The parameter d_{mode} approximately corresponds to the maximum of grain size distribution. The two latter parameters represent the lower and upper limits of grain size in a sample, so that, subjectively, approximately 95% of all the grains in a sample fall between d_{lower} and d_{upper}. The size of acicular grains in sample M0.35 is measured along their long axes. Only d_{mode} was estimated for natural (NR) samples. Abbreviations: T_V, the Verwey transition temperature; H_c, coercivity; H_{cr}, coercivity of remanence; M_{rs}, saturation remanence; and M_s, saturation magnetization. The R_{LT} ratio is defined in the text.

Sample	d_{mode} (μm)	d_{lower} (μm)	d_{upper} (μm)	T_V (K)	M_{rs}/M_s	H_{cr}/H_c	R_{LT}
M0.35 (acicular)	0.35	0.2	0.5	112	0.351	1.47	1.27
M0.15	0.15	0.03	0.6	108	0.208	2.02	1.12
M0.25	0.25	0.1	0.5	116	0.192	1.99	1.09
M0.75	0.75	0.3	2.75	118	0.175	2.05	1.02
M1.5	1.5	0.5	6.5	114	0.144	2.29	1.01
M5	5	2	10	120	0.105	2.6	0.93
M12	12	4	20	117	0.062	3.45	0.77
M30	30	10	60	116	0.044	3.77	0.67
M100	100	40	200	114	0.021	6.86	0.58
NR1	$\sim$1–2	n/a	n/a	115	0.131	2.24	1.03
NR2	$\sim$20–30	n/a	n/a	118	0.05	3.4	0.68
NR3	$<$100 nm	n/a	n/a	119	0.304	1.53	1.31

The character of this control, however, depends on magnetic domain state (and, hence, on the grain size and shape) of magnetite (e.g., Kosterov, 2001; Smirnov and Tarduno, 2002; Carter-Stiglitz *et al*., 2006). In particular, magnetic domain state affects the ratio (R_{LT}) between an SIRM imparted at a very low temperature (10–20 K) after cooling in a strong magnetic field ($>$1 T) (field cooling, FC) and an SIRM imparted after cooling in a zero field environment (zero field cooling, ZFC). For single-domain (SD) magnetite, the FC SIRM is always greater than the ZFC SIRM (e.g., Moskowitz *et al*., 1993; Carter-Stigliz *et al*., 2002). In contrast, for large multidomain (MD) magnetite grains, the FC SIRM has been found to be significantly lower than the ZFC SIRM (e.g., Kosterov, 2001; Brachfeld *et al*., 2002; Carter-Stiglitz *et al*., 2006). Such a difference in the R_{LT} ratio reflects different mechanisms governing the SIRM acquisition in single-domain and multidomain magnetite below T_V (Kosterov, 2003).

However, the evolution of R_{LT} ratio between the two extreme cases representing SD and MD magnetite grains remains largely unknown. Unfortunately, only two data points are currently available for pseudo-single domain (PSD) magnetite, both showing nearly equal ZFC and FC SIRMs (Smirnov and Tarduno, 2002; Kosterov, 2003). Further accumulation of experimental data for PSD magnetites, therefore, may be important for better understanding the magnetization processes in monoclinic magnetite.

In this brief paper, I report the results of experimental study of the R_{LT} ratio as a function of the mean grain size for polycrystalline nearly-stoichiometric synthetic magnetite, with an emphasis on pseudo-single domain state. The R_{LT} ratio was also measured from natural magnetite-bearing volcanic rocks, representing SD, PSD, and MD states. Finally, I briefly discuss implications of the obtained data for understanding the mechanisms governing magnetic properties of magnetite below the Verwey transition.

2. Samples

2.1 Synthetic magnetite

Nine samples of synthetic polycrystalline magnetite were studied (Table 1). Before measurements, the samples were reduced in a CO/CO_2 (1:10) atmosphere at 400°C for 3–16 hours to obtain nearly stoichiometric magnetite. The mass-normalized saturation magnetization (M_s^{norm}) measured at room temperature after thermal treatment ranged between 85 and 90 A m^2/kg, indicating almost complete conversion to pure magnetite (e.g., Stacey and Banerjee, 1974).

The grain size and shape distributions of synthetic samples were determined by visual inspection of images obtained using a low-voltage, high-resolution LEO 982 scanning electron microscope (SEM) at the University of Rochester, an XL-30 Environmental SEM at Yale University, or JEOL JSM-6400 SEM at Michigan Technological University. In all but one sample, magnetite grains were characterized by irregular, nearly equidimensional shape. One sample (M0.35) contained elongate grains with aspect ratio ranging between $\sim$1:6 and 1:12. The grain-size distributions for all samples studied are well approximated log-normally.

To characterize magnetic domain state of the samples, magnetic hysteresis properties (saturation magnetization, M_s; saturation remanence, M_{rs}; coercivity, H_c; coercivity of remanence, H_{cr}) were measured at room temperature (Table 1), using a Princeton Measurements variable-temperature vibrating sample magnetometer at the Institute of Rock Magnetism (The University of Minnesota) or a Princeton Measurement alternating gradient force magnetometer at the University of Rochester and Michigan Technological University. All room temperature hysteresis loops have a regular shape (Fig. 1(a)) suggesting unimodal grain-size distributions and single mineral compositions (e.g., Tauxe *et al.,* 1996).

The hysteresis data indicate various magnetic domain behavior of the studied samples (Fig. 1(c)). Sample M0.35 plots closest to the SD region of the Day-Dunlop plot (Day *et al.,* 1977; Dunlop, 2002). Grains in this sample are larger

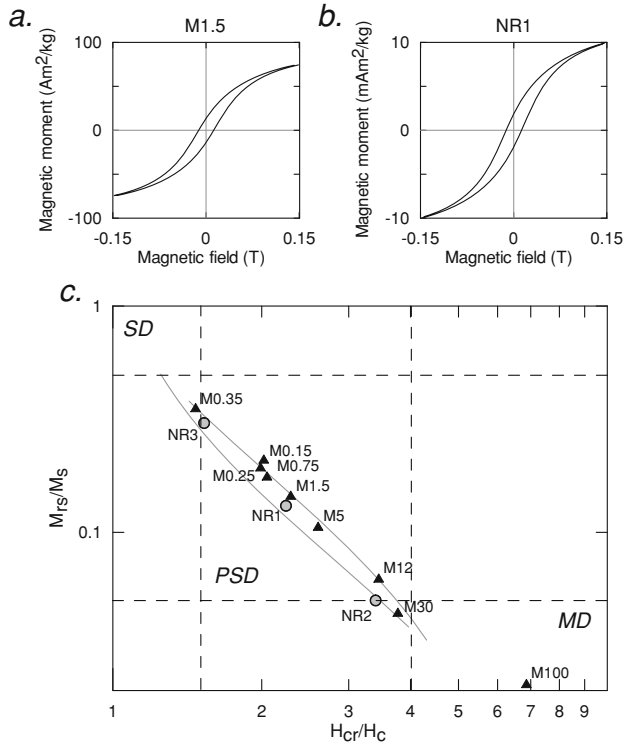

Fig. 1. (a, b) A closeup view of the central part of the mass-normalized magnetic hysteresis loop measured at room temperature from the samples M1.5 (a) and NR1 (b) (the maximum field of magnetic hysteresis measurement was 1.5 T). (c) Day-Dunlop plot (Day *et al*., 1977; Dunlop, 2002). Synthetic and natural samples are shown by solid triangles and gray circles, respectively. Abbreviations are H_c, coercivity; H_{cr}, coercivity of remanence; M_{rs}, saturation remanence; and M_s, saturation magnetization; SD, single domain; PSD, pseudo-single domain; MD, multidomain. Also shown by grey lines are SD-MD mixture models from Dunlop (2002).

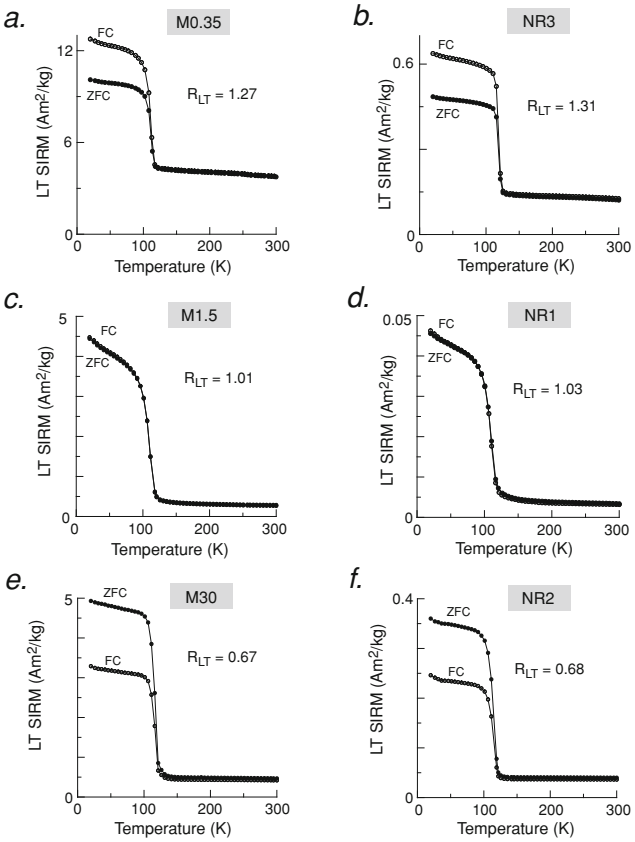

Fig. 2. Thermal demagnetization of low-temperature saturation isothermal remanent magnetization (LT SIRM) imparted at 20 K after cooling in a zero field environment (solid symbols) and in a 2.5 T magnetic field (open symbols) for nearly single-domain samples M0.35 (a) and NR3 (b), pseudo-single domain samples M1.5 (c) and NR1 (d), and multidomain samples M30 (e) and NR2 (f).

than the SD threshold for magnetite (0.05–0.06 μm; Dunlop and Özdemir, 1997), so their nearly SD state is likely defined by the dominant role of shape anisotropy in the elongate particles. The M_{rs}/M_s ratio for this sample is lower than the expected theoretical value for non-interacting uniaxial SD grains (0.5), most likely due to magnetostatic interactions between grains (Sprowl, 1990) or the presence of larger grains in the sample. Samples M0.15, M0.25, M0.75, M1.5, and M5.0 manifest pseudo-single domain hysteresis behavior, while samples M12, M30, and M100 plot close to or within the MD region of the Day-Dunlop diagram (Fig. 1(c), Table 1).

2.2 Natural rock (NR) samples

In addition to the synthetic samples, three natural magnetite-bearing samples were studied. The opaque mineralogy of the samples was investigated on polished thin sections using scanning electron microscopy. The compositions of oxide grains were determined by means of energy dispersive spectrometry (EDS).

The first sample (NR1) represents a ∼2.45 Ga Matachewan mafic dike (Smirnov and Tarduno, 2004). Over 95% of the oxide minerals present were relatively large (several hundreds of microns to >1 mm) grains, containing one or several subordinate sets of trellis type lamellae (e.g., Haggerty, 1991). Between the lamellae, fine (from submicron to 2–3 μm in size) intergrowths of two phases were observed. SEM and low-temperature magnetic analyses indicated that these phases are nearly stoichiometric magnetite and ilmenite produced by oxyexsolution (Smirnov and Tarduno, 2005). The sample manifests PSD hysteresis behavior (Fig. 1(b), (c); Table 1), consistent with SEM data. Magnetic hysteresis loops measured from this (Fig. 1(b)) and the other natural samples are of a regular shape, indicating unimodal grain size distributions.

The second sample (NR2) represents a gabbrodolerite supposedly from ∼2.44 Ga Widgiemooltha dike swarm (Smirnov and Evans, 2006). The SEM imaging demonstrates the presence of large magnetite grains with the mean size of 20–40 μm. Although the magnetite-ilmenite intergrowth is common in other dikes of this swarm, it is not observed for this sample. The multidomain magnetic state of NR2 is indicated by magnetic hysteresis data (Fig. 1(c); Table 1).

The third sample (NR3) represents a mafic dike cutting through the ∼3.2 Ga Kaap Valley Pluton. Backscattered electron imaging suggest the presence of fine scale Ti-poor and Ti-rich intergrowth, but their very small size (<100 nm) prevents exact determination of their composition by conventional EDS analysis. However, the well expressed Verwey transition (Fig. 2(b)) strongly supports the presence

of magnetite as the "Ti-poor" mineral phase. These small magnetite subvolumes are approximately equidimensional. Magnetic hysteresis behavior of this sample suggests its nearly single-domain magnetic state (Fig. 1(c); Table 1).

3. Experimental Procedure and Results

Low-temperature magnetic measurements were performed using a Quantum Design Magnetic Property Measurement System (MPMS). Before measurements, a sample was demagnetized along three orthogonal axes in an alternating magnetic field of 0.2 T at room temperature (300 K). After, it was cooled to 20 K in a zero magnetic field (ZFC). At 20 K, a saturating isothermal remanent magnetization (ZFC SIRM) was imparted in a 2.5 T magnetic field. The field was applied for 60 s, after which the superconducting magnet was immediately quenched (reset) to reduce the residual field to <1 μT. Thermal demagnetization of the ZFC SIRM was measured at 5 K intervals during zero field warming to 300 K. The sample was next cooled from 300 K to 20 K in the presence of a 2.5 T magnetic field. At 20 K, a saturation remanence (FC SIRM) was induced by keeping a sample in a 2.5 T magnetic field for 60 s. After quenching the magnet, the thermal demagnetization of FC SIRM was measured between 20 and 300 K. All studied samples are characterized by well expressed sharp Verwey transition at 108–120 K (Table 1), characteristic of nearly stoichiometric magnetite.

For each sample, the ratio:

$$R_{\mathrm{LT}} = \frac{\mathrm{FC\ \ SIRM\,(20\,K)}}{\mathrm{ZFC\ \ SIRM\,(20\,K)}} \qquad (1)$$

was calculated (Table 1). The ratio manifests a noticeable dependence on magnetic domain state (Figs. 2 and 3).

A significant elevation of FC SIRM over ZFC SIRM is observed for nearly single-domain sample M0.35 ($R_{\mathrm{LT}} = 1.27$; Fig. 2(a)). Its R_{LT} ratio is practically identical to those reported for biogenic SD magnetite ($R_{\mathrm{LT}} = 1.24$; Moskowitz *et al.*, 1993) and SD magnetite inclusions in plagioclase phenocrysts from the Lambertville diabase ($R_{\mathrm{LT}} = 1.25$; Carter-Stiglitz *et al.*, 2002). The natural sample NR3 shows only a slightly higher ratio $R_{\mathrm{LT}} = 1.31$ (Fig. 2(b)).

The R_{LT} ratio for the pseudo-single domain synthetic magnetites (M0.15, M0.25, M0.75, M1.5, and M5.0) is close to unity (e.g., Fig. 2(c)), slightly decreasing with increasing grain size from $R_{\mathrm{LT}} = 1.12$ for M0.15 to $R_{\mathrm{LT}} = 0.93$ for M5. A similar close-to-unity ratio ($R_{\mathrm{LT}} = 1.03$) is also observed for the sample NR1 characterized by pseudo-single domain magnetic hysteresis behavior (Fig. 2(d)).

For the synthetic samples containing larger multidomain grains (M12, M30, and M100), FC SIRM is much weaker than ZFC SIRM (e.g., Fig. 2(e)). As a result, the R_{LT} ratios plot significantly below unity, decreasing from $R_{\mathrm{LT}} = 0.77$ for M12 to $R_{\mathrm{LT}} = 0.58$ for M100. The natural MD sample NR2 is characterized by $R_{\mathrm{LT}} = 0.68$ (Fig. 2(f)).

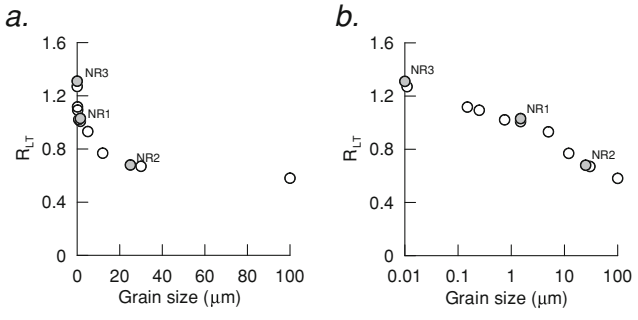

Fig. 3. (a) Grain-size dependence of the R_{LT} ratio for synthetic magnetites (open circles) and natural magnetite-bearing samples (gray circles). Note that a tentative mean grain-size of 0.01 μm is used for the sample M0.35 to reflect its nearly single-domain state. (b) The same data plotted against logarithmic scale along the grain size axis.

4. Discussion and Conclusions

The experimental results described above are consistent with the results of prior studies of synthetic magnetites (Kosterov, 2001, 2003; Smirnov and Tarduno, 2002; Carter-Stiglitz *et al.*, 2006), biogenic magnetite (Moskowitz *et al.*, 1993) and natural magnetite-bearing samples (Brachfeld *et al.*, 2001, 2002; Carter-Stiglitz *et al.*, 2002, 2006).

The elevation of FC SIRM over ZFC SIRM observed for the samples manifesting nearly SD magnetic behavior can be explained by the following simple model (e.g., Bickford, 1950; Williams *et al.*, 1953). In the absence of external enforcement (e.g., a magnetic field) during cooling, the monoclinic c-axis may develop in any of the cube-edge orientations with equal probability. Hence, the distribution of easy magnetization axes after ZFC is random. However, application of a strong magnetic field (>100 mT) during cooling sets all c-axes along the cubic [001] direction closest to the magnetic field (e.g., Calhoun, 1954). As a result, easy magnetization axes after FC would be uniformly distributed within the cone with a conical angle of 54.73° around the cooling field direction (e.g., Kosterov, 2001). Such an alignment of easy axes results in more intense low-temperature SIRM after field cooling and, hence, $R_{\mathrm{LT}} > 1$.

In contrast, three multidomain synthetic magnetite samples show a significant elevation of ZFC SIRM over FC SIRM (Fig. 3). To explain such a behavior, Kosterov (2003) proposed an elegant extension of the field-induced c-axes alignment model for multidomain grains. He pointed out that microcoercivities in MD grains due to domain walls displacement vary as $H_{\mathrm{c0}}/\cos\theta$, where θ is the angle between the domain magnetization and the external field, and H_{c0} is a critical field for $\theta = 0$. Therefore, the bulk coercive force, H_{c}, is higher for a grain ensemble in which relatively larger fraction of grains have easy magnetization axes directed at large angles with respect to the external field (that is $H_{\mathrm{c}}^{\mathrm{ZFC}} > H_{\mathrm{c}}^{\mathrm{FC}}$). Because in MD grains saturation remanence is related to coercivity through the demagnetizing factor (SIRM $\propto H_{\mathrm{c}}/N$; e.g., Dunlop and Özdemir, 1997), ZFC SIRM will be larger than FC SIRM, resulting in $R_{\mathrm{LT}} < 1$. Recently, Carter-Stiglitz *et al.* (2006) convincingly argued that, in addition to Kosterov's "geometrical" mechanism, higher coercivity of MD grains after zero field cooling can be caused by the presence of "hard" magnetic 90°-domain walls associated with twin boundaries (at which two c-axes are perpendicular).

For pseudo-single domain synthetic magnetites, the R_{LT} ratio is close to unity (Fig. 3). It is unlikely to be a result of simple mixing of the signals from sub-ensembles of true SD

and true MD grains, the R_{LT} ratio of each being governed by one of the mechanisms described above. Although the PSD samples are characterized by relatively wide grain size distributions, the latter are unimodal and do not contain any significant amount of SD grains (cf. Smirnov, 2006). I note that the mean grain size of all studied samples is larger than the SD threshold ($d_{SD} \approx 0.14$ μm) for magnetite below the Verwey transition suggested by micromagnetic modelling (Muxworthy and Williams, 1999).

For the R_{LT} ratio to become close to unity, the M_{rs}/M_s ratio of a magnetite grain ensemble after field cooling should be close to that after zero field cooling. Let us consider the evolution of ZFC and FC state with decreasing grain size separately. After ZFC, a magnetic grain will be divided into twin domains. While there is no theoretical or direct experimental constraint on the grain size below which twinning would not be energetically favorable, some indirect data hint that twins may form in grains as small as 0.15 μm (Smirnov, 2006). Hence it is reasonable to suggest that, as the grain size becomes smaller (starting from a large MD grain), the number of magnetic domain walls in each twin decreases and, eventually, at some grain size d_{crit} ($> d_{SD}$), each twin domain effectively behaves as an SD particle (i.e. containing no magnetic domain walls). Correspondingly, the M_{rs}/M_s ratio will increase with decreasing grain size, until it reaches an SD value (at d_{crit}) and remains more or less constant with a further decrease of grain size.

On the other hand, cooling in a strong magnetic field prevents twinning and, hence, twin boundaries do not affect the processes of remagnetization by displacement of magnetic domain walls. In addition, the effective grain size of FC state will be larger than that of ZFC state (assuming that some twins may behave as independent magnetic grains). Therefore, the FC state should remain "softer" than the ZFC state (hence, FC SIRM $<$ ZFC SIRM) until the whole grain becomes single-domain after field cooling. If the M_{rs}/M_s ratio of FC state is entirely defined by the MD mechanism (Kosterov, 2003), it should remain lower than its counterpart for ZFC state for all grain sizes, until a grain is single-domain after FC. However, this is not consistent with the experimental observations presented here, which show that FC SIRM $\approx$ ZFC SIRM within a relatively wide grain size range.

To explain such a behavior, I speculate that, by analogy with PSD grains at room temperature, some SD-like component may exist in the magnetization of small MD grains below T_V, over and above their "normal" MD remanence (Dunlop and Özdemir, 1997). While the concrete physical mechanism of such a component is unclear, it may originate from the presence of truly SD moments, which can reverse independently of surrounding domains (e.g., Dunlop, 1973) or metastable SD grains in which walls have failed to nucleate following saturation (e.g., Halgedahl and Fuller, 1983). Independent of its origin, the SD-like component will result in a higher M_{rs}/M_s ratio of the FC state within a certain grain size range. The results presented here hint that these "anomalously" high FC SIRM may appear in grains smaller than $\sim$5 μm. This change in the remanence acquisition mode may be reflected by the point of inflection in Fig. 3(b) around $\sim$5 μm. In addition, with decreasing grain size, the alignment of easy magnetization axes may play an increasing role in defining the FC SIRM intensity. As a result of these processes, FC SIRM gradually approaches ZFC SIRM from below as grain size decreases and eventually exceeds it. This may explain a monotonic increase in the R_{LT} ratio between samples with the 5 μm and 0.15 μm mean grain sizes.

For grains, so small that they are single-domain after FC, their R_{LT} ratio is solely defined by the difference in easy axes alignments after ZFC and FC. The results presented here indicate that the transition between the SD and MD mechanisms of SIRM acquisition is gradual rather than stepwise. However, it is important to emphasize that, the R_{LT} ratios presented in this paper are integrated values representing grain size distribution within each sample. A higher resolution of the grain size dependence of R_{LT} can be obtained only by using samples characterized by narrow grain size distributions and well-controlled stoichiometry, grain shape and spacing (e.g., King *et al.,* 1996). Recent advances in nanoengineering make the fabrication of such samples achievable in the nearest future (e.g., Wang *et al.,* 2004; Kong *et al.,* 2008).

On a more practical side, the R_{LT} ratios obtained for synthetic magnetite may be used as a baseline for crude estimation of magnetic domain state in some natural samples. Naturally, such an approach can only be used for rocks containing nearly stoichiometric magnetite, for example, resulting from oxyexsolution in mafic dikes. The presence of other mineral phases, which may become ferromagnetic at low temperatures may complicate the calculation of R_{LT}, although the magnetite component is likely to be dominant because of very strong magnetocrystalline anisotropy at cryogenic temperatures. The potential usefulness of this approach has been demonstrated by Brachfeld *et al.* (2001, 2002) who were able to identify multidomain magnetite in glaciomarine sediments from the western Antarctic Peninsula.

Acknowledgments. I am grateful to Andrei Kosterov for valuable discussions. I also appreciate the helpful reviews by Ö. Özdemir and D. Krása. I thank the Institute for Rock Magnetism (University of Minnesota) for Visiting Fellowships. Funds for the IRM are provided by the National Science Foundation (NSF) Instruments and Facilities Program and by the University of Minnesota.

References

Arkani-Hamed, J., On the possibility of single-domain/pseudo-single-domain magnetic particles existing in the lower crust of Mars: Source of the strong magnetic anomalies, *J. Geophys. Res.*, **110**, E12009, doi:10.1029/2005JE002535, 2005.

Bickford, L. R., Jr., Ferromagnetic resonance absorption in magnetite single crystals, *Phys. Rev.*, **78**, 449–457, 1950.

Brachfeld, S. A., Y. Guyodo, and G. D. Acton, The magnetic mineral assemblage of hemipelagic drifts, ODP Site 1096, in *Proc. ODP Sci. Results 178*, edited by Barker, P. F., Camerlenghi, A., Acton, G. D., and Ramsay, A. T. S., 1–12, 2001.

Brachfeld, S. A., S. K. Banerjee, Y. Guyodo, and G. D. Acton, A 13200 year history of century to millennial-scale paleoenvironmental change magnetically recorded in the Palmer Deep, western Antarctic Peninsula, *Earth Planet. Sci. Lett.*, **194**, 311–326, 2002.

Calhoun, B. A., Magnetic and electric properties of magnetite at low temperatures, *Phys. Rev.*, **94**, 1577–1585, 1954.

Carter-Stiglitz, B., M. Jackson, and B. Moskowitz, Low-temperature remanence in stable single domain magnetite, *Geophys. Res. Lett.*, **29**, doi:10/1029/2001GL014197, 2002.

Carter-Stiglitz, B., B. Moskowitz, P. Solheid, T. S. Berquó, M. Jackson, and A. Kosterov, Low-temperature magnetic behavior of multidomain titanomagnetites: TM0, TM 16, and TM35, *J. Geophys. Res.*, **111**, B12S05, doi:10.1029/2006JB004561, 2006.

Chikazumi, S., K. Chiba, K. Suzuki, and T. Yamada, Electron microscopic observation of low temperature phase of magnetite, in *Ferrites: Proceedings of the International Conference*, edited by Y. Hoshino, S. Iida, and M. Sugimoto, pp. 141–143, University of Tokyo Press, Tokyo, 1971.

Day, R., M. Fuller, and V. A. Schmidt, Hysteresis properties of titanomagnetites: Grain-size and compositional dependence, *Phys. Earth Planet. Inter.*, **13**, 260–267, 1977.

Dunlop, D. J., Superparamagnetic and single-domain threshold sizes in magnetite, *J. Geophys. Res.*, **78**, 1780–1793, 1973.

Dunlop, D. J., Theory and application of the Day plot (M_{rs}/M_s versus H_{cr}/H_c) 1. Theoretical curves and tests using titanomagnetite data, *J. Geophys. Res.*, **107**, EPM4, 2002.

Dunlop, D. J. and Ö. Özdemir, *Rock Magnetism: Fundamentals and Frontiers*, 573 pp., Cambridge Univ. Press, Cambridge, 1997.

Geiss, C. E., C. W. Zanner, S. K. Banerjee, and M. Joanna, Signature of magnetic enhancement in a loessic soil in Nebraska, United States of America, *Earth Planet. Sci. Lett.*, **228**, 355–367, 2004.

Haggerty, S. E., Oxide textures—A mini-atlas, *Rev. Mineral.*, **25**, 129–219, 1991.

Halgedahl, S. L. and M. Fuller, The dependence of magnetic domain structure upon magnetization state with emphasis on nucleation as a mechanism for pseudo-single-domain behavior, *J. Geophys. Res.*, **88**, 6505–6522, 1983.

Halgedahl, S. L. and R. D. Jarrard, Low-temperature behavior of single-domain through multidomain magnetite, *Earth Planet. Sci. Lett.*, **130**, 127–139, 1995.

Kakol, Z., Magnetic and transport properties of magnetite in the vicinity of the Verwey transition, *J. Solid Stat. Chem.*, **88**, 104–114, 1990.

King, J. G., W. Williams, C. D. W. Wilkinson, S. McVitie, and J. N. Chapman, Magnetic properties of magnetite arrays produced by the method of electron beam lithography, *Geophys. Res. Lett.*, **23**, 2847–2850, 1996.

Kirschvink, J. L. and H. A. Lowenstam, Mineralization and magnetization of chiton teeth: Paleomagnetic, sedimentologic, and biologic implications of organic magnetite, *Earth Planet. Sci. Lett.*, **44**, 193–204, 1979.

Kong, X., D. Krása, H. P. Zhou, W. Williams, S. McVitie, J. M. R. Weaver, and C. D. W. Wilkinson, Very high resolution etching of magnetic nanostructures in organic gases, *Microelec. Eng*, doi:10.1016/j.mee.2007.12.006, 2008 (in press).

Kopp, R. E., T. D. Raub, D. Schumann, H. Vali, A. V. Smirnov, and J. L. Kirschvink, Magnetofossil spike during the Paleocene-Eocene thermal maximum: Ferromagnetic resonance, rock magnetic, and electron microscopy evidence from Ancora, New Jersey, United States, *Paleoceanography*, **22**, doi:10.1029/2007PA001473, 2007.

Kosterov, A. A., Magnetic hysteresis of pseudo-single-domain and multidomain magnetite below the Verwey transition, *Earth Planet. Sci. Lett.*, **186**, 245–253, 2001.

Kosterov, A. A., Low-temperature magnetization and AC susceptibility of magnetite: effect of thermomagnetic history, *Geophys. J. Int.*, **154**, 58–71, 2003.

Li, C. H., Magnetic properties of magnetite crystals at low temperature, *Phys. Rev.*, **40**, 1002–1012, 1932.

Medrano, C., M. Schlenker, J. Baruchel, J. Espeso, and Y. Miyamoto, Domains in the low-temperature phase of magnetite from synchrotron-radiation x-ray topographs, *Phys. Rev. B.*, **59**, 1185–1195, 1999.

Moskowitz, B. M., R. B. Frankel, and D. A. Bazylinski, Rock magnetic criteria for the detection of biogenic magnetite, *Earth Planet. Sci. Lett.*, **120**, 283–300, 1993.

Muxworthy, A. R. and W. Williams, Micromagnetic models of pseudo-single-domain grains of magnetite near the Verwey transition, *J. Geophys. Res.*, **104**, 29203–29217, 1999.

Özdemir, Ö. and D. J. Dunlop, Low-temperature properties of a single crystal of magnetite oriented along principal magnetic axes, *Earth Planet. Sci. Lett.*, **165**, 229–239, 1999.

Özdemir, Ö., D. J. Dunlop, and B. M. Moskowitz, The effect of oxidation on the Verwey transition in magnetite, *Geophys. Res. Lett.*, **20**, 1671–1674, 1993.

Özdemir, Ö., D. J. Dunlop, and B. M. Moskowitz, Changes in remanence, coercivity, and domain state at low temperature in magnetite, *Earth Planet. Sci. Lett.*, **194**, 343–358, 2002.

Schmidbauer, E. and R. Keller, Magnetic properties and rotational hysteresis of Fe_3O_4 and g-Fe_2O_3 particles ∼250 nm in diameter, *J. Magn. Magn. Mater.*, **152**, 99–108, 1996.

Smirnov, A. V., Memory of the magnetic field applied during cooling in the low-temperature phase of magnetite: Grain-size dependence, *J. Geophys. Res.*, **111**, B12S04, doi10.1029/2006JB004573, 2006.

Smirnov, A. V. and J. A. Tarduno, Magnetic field control of the low-temperature magnetic properties of stoichiometric and cation-deficient magnetite, *Earth Planet. Sci. Lett.*, **194**, 359–368, 2002.

Smirnov, A. V. and J. A. Tarduno, Secular variation of the Late Archean–Early Proterozoic geodynamo, *Geophys. Res. Lett.*, **31**, L16607, doi:10.1029/2004GL020333, 2004.

Smirnov, A. V. and J. A. Tarduno, Thermochemical remanent magnetization in Precambrian rocks: Are we sure the geomagnetic field was weak?, *J. Geophys. Res.*, **110**, doi:10.1029/2004JB003445, B06103, 2005.

Smirnov, A. V. and D. A. D. Evans, Paleomagnetism of the ∼2.4 Ga Widgiemooltha Dike Swarm (Western Australia): Preliminary Results, *Eos Trans. AGU*, **87(36)**, Jt. Assem. Suppl., Abstract GP23A-01, 2006.

Sprowl, D. R., Numerical estimation of interactive effects in single-domain magnetite, *Geophys. Res. Lett.*, **17**, 2009–2012, 1990.

Stacey, F. D. and S. K. Banerjee, *The physical principles of rock magnetism*, 195 pp., Elsevier, Amsterdam, 1974.

Syono, Y., Magnetocrystalline anisotropy and magnetostriction of Fe_3O_4-Fe_2TiO_4 series—with special application to rock magnetism, *Jap. J. Geophys.*, **4**, 71–143, 1965.

Tauxe, L., T. A. T. Mullender, and T. Pick, Potbellies, wasp-waists, and superparamagnetism in magnetic hysteresis, *J. Geophys. Res.*, **101**, 571–583, 1996.

Verwey, E. J. W., Electron conduction of magnetite (Fe_3O_4) and its transition point at low temperatures, *Nature*, **144**, 327–328, 1939.

Wang, J., Z. M. Peng, Y. J. Huang, and Q. W. Chen, Growth of magnetite nanorods along its easy-magnetization axis of [110], *J. Cryst. Growth*, **263**, 616–619, 2004.

Williams, H. J., R. M. Bozorth, and M. Goertz, Mechanism of transition in magnetite at low temperatures, *Phys. Rev.*, **91**, 1107–1115, 1953.

Zuo, J. M., J. C. H. Spence, and W. Petuskey, Charge ordering in magnetite, *Phys. Rev. B*, **42**, 8451–8464, 1990.

A. V. Smirnov (e-mail: asmirnov@mtu.edu)